

The drag coefficient, bottom roughness, and wave-breaking in the nearshore

Falk Feddersen¹, E. L. Gallagher², R. T. Guza³, and Steve Elgar¹

Short title: THE DRAG COEFFICIENT IN THE NEARSHORE

¹Woods Hole Oceanographic Institution, Woods Hole, Massachusetts.

²Naval Postgraduate School, Monterey, California

³Center for Coastal Studies, Scripps Institution of Oceanography, La Jolla, California

Abstract. The bottom drag coefficient in the nearshore has been suggested to depend on bottom roughness (bedforms) or alternatively on wave breaking. The hypothesis that bottom drag coefficient depends on bottom roughness is tested with two months of field observations collected on a sandy ocean beach during the Duck94 field experiment. Both the drag coefficient (estimated from alongshore momentum balances) and bottom roughness (estimated from fixed altimeters) are larger within the surfzone than in the region farther seaward. Although the drag coefficient increases with roughness seaward of the surfzone, no relationship was found between the drag coefficient and roughness related quantities within the surfzone. These results suggest that breaking-wave generated turbulence increases the surfzone drag coefficient.

Keywords: Nearshore, Bed Roughness, Drag Coefficient, Circulation

1. Introduction

The mean (time-averaged) bottom stress is an important component of nearshore circulation and sediment transport dynamics. In depth-integrated circulation models, the mean alongshore bottom stress τ_b^y often is written as

$$\tau_b^y = \rho c_d \langle |\vec{u}|v \rangle \quad (1)$$

where ρ is the water density, c_d is the non-dimensional drag coefficient, and $\langle \cdot \rangle$ represents a time average over many wave periods. The horizontal velocity vector \vec{u} and the alongshore velocity v include both mean and wave components, above the bottom boundary layer. In nearshore circulation models, $\langle |\vec{u}|v \rangle$ can be represented well with low-order moments of the velocity field [Fedderson *et al.*, 2000], and thus accurate parameterizations of c_d are required to model the bottom stress.

The bottom stress is equal to the turbulent vertical flux of horizontal momentum into a viscous bottom boundary layer, i.e., for the alongshore bottom stress,

$$\tau_b^y = -\rho \langle v'w' \rangle \quad (2)$$

where v' and w' are the turbulent alongshore and vertical velocities, respectively. Therefore, c_d depends on the turbulence, and for constant $\langle |\vec{u}|v \rangle$, c_d increases with increased turbulence levels. Both of the two primary sources of nearshore turbulence, shear in the bottom boundary layer [e.g., Grant and Madsen, 1979], and the breaking of surface gravity waves [e.g., Svendsen, 1987], have been proposed to affect c_d [e.g., Fredsoe and Deigaard, 1992; Van Rijn, 1993]. For simplicity, many nearshore circulation models have assumed a spatially

constant c_d [Longuet-Higgins, 1970; Özkan-Haller and Kirby, 1999, and many others], with the value of c_d usually determined by fitting to observations.

On the continental shelf, breaking wave generated turbulence does not reach the lower part of the water column and thus does not influence the bottom boundary layer. *Grant and Madsen* [1979] generalized the Prandtl-Karman law of the wall to the continental shelf bottom boundary layer in the presence of wave-orbital velocities and bottom roughness, i.e.,

$$\bar{v}(z) = \frac{\bar{v}_*}{\kappa} \log\left(\frac{z}{z_a}\right), \quad (3)$$

where z is the height above the bottom, z_a is the apparent roughness height that depends on waves and bottom roughness, and κ is von Karman constant. The current friction velocity \bar{v}_* is defined so that

$$\tau_b^y = \rho \bar{v}_*^2. \quad (4)$$

Garcez-Faria et al. [1998] used this model to estimate the alongshore bottom stress in the nearshore (depths < 4 m) by fitting alongshore current observations that spanned much of the water column to a log profile (3), and solved for c_d using (4) and (1). *Garcez-Faria et al.* [1998] found that c_d was related to the root-mean-square bottom roughness normalized by water depth k_{rms}/h with correlation $r = 0.63$, and that c_d was inversely proportional to the percentage of waves breaking. In contrast, *Fredsoe and Deigaard* [1992] and *Church and Thornton* [1993] hypothesized that differences in c_d within and seaward of the surfzone are caused by differences in breaking-wave turbulence levels, with increased breaking resulting in larger c_d . *Feddersen et al.* [1998] found larger (by factor of 3) c_d within the surfzone relative to seaward of the surfzone, but it was unclear whether this c_d variation resulted from differences

in bottom roughness or wave breaking.

Here, the dependence of nearshore c_d on bottom roughness and wave breaking is examined further using two months of observations acquired on a sandy ocean beach. Bottom roughness observations [Gallagher *et al.*, 1998a] obtained concurrently with wave and current observations [Feddersen *et al.*, 1998] are used to estimate spatial averages of roughness quantities (k_{rms} and k_{rms}/h) and c_d , as described in section 2. Although c_d and roughness variables are consistently larger within the surfzone than seaward of the surfzone, no relationship is observed between c_d and roughness variables within the surfzone (section 3). This suggests that in these observations the elevated surfzone c_d likely is influenced more strongly by breaking-wave generated turbulence than by elevated bottom roughness, consistent with the hypothesis of Fredsoe and Deigaard [1992] and Church and Thornton [1993]. Reasons these results differ from those of Garcez-Faria *et al.* [1998], in particular the limitations of the methods used here and of the log-profile approach (3) in the surfzone, are discussed in section 4.

2. Observations and Methods

Observations were obtained during the Duck94 field experiment (September–October, 1994) near Duck, North Carolina. Pressure sensors, bidirectional current meters, and altimeters, sampled at 2 Hz, were deployed on a cross-shore transect (Figure 1) extending 750 m from near the shoreline to 8-m water depth [Gallagher *et al.*, 1998a; Feddersen *et al.*, 1998].

Figure 1.

Roughness Estimates

The altimeters measure acoustically the distance to the seafloor from a fixed frame. At each altimeter, the 2 Hz data were processed into 32-s bed-location estimates (e.g., Figure 2) [Gallagher *et al.*, 1996], that were demeaned and detrended to produce 24-hr root-mean-square (rms) bed roughness k_{rms} estimates. Bed roughness normalized by water depth k_{rms}/h also was estimated every 24 hours, using the 24-hr average water depth h .

Figure 2.

This k_{rms} estimation method assumes that the bedforms migrate under the altimeter so that time variability approximates spatial variability. If either the roughness field is frozen or if the bed erodes or accretes uniformly in space (at time scales not removed by detrending), this method fails. The k_{rms} estimates are believed accurate for the following reasons. First, coherently migrating bedforms were observed 60% of the time under a 1.4 m by 1.4 m altimeter array co-deployed 70 m from the shoreline [Gallagher *et al.*, 1998b], supporting the assumption that time variability approximates spatial variability. For most of the remaining 40% of the time, k_{rms} was small. Second, the magnitude and variability of k_{rms} in the cross-shore (Figure 3) is consistent with spatial-series based k_{rms} observations occasionally collected during this experiment [Thornton *et al.*, 1998]. The mean and variability of k_{rms} are largest within 100 m of the shoreline (where the surfzone usually is located) and decay farther offshore. Third, towed and fixed altimeter k_{rms} estimates agree well within and seaward of the surfzone at the same beach during an experiment three years later (not shown).

Figure 3.

Spatially weighted (i.e., integral) averages of k_{rms} and k_{rms}/h were calculated on the transect within and seaward of the surfzone (Figure 1). The cross-shore extent of the surfzone

(averaged over 24 hours) was estimated heuristically based on energy flux relative to the flux in 8-m depth, the local energy flux gradient, and time-lapsed video images (R. A. Holman, personal communication, 1996) as described in *Feddersen et al.* [1998]. The 24-hr k_{rms} are significantly ($> 98\%$) correlated at cross-shore lags up to 125 m, indicating that the cross-shore k_{rms} variability is not dominated by unresolved short spatial scales that would cause errors in the spatial averages. The 24-hr averaged roughness quantities (k_{rms} and k_{rms}/h) for the full-transect, the surfzone, and seaward of the surfzone were averaged into 48-hr estimates for comparison with c_d estimates.

Bedform lengthscales and orientation cannot be determined from these altimeter observations. During the same experiment, the dominant horizontal spatial scales of bed variability were in the range 1–5 m [*Thornton et al.*, 1998; *Gallagher et al.*, 1998b], similar to the observed wave-orbital diameters (1–4 m). The altimeter-estimated k_{rms} are assumed to correspond to the bedforms with these lengthscales. The orientation of long-crested bedforms relative to a steady current can have a significant effect on the bottom stress [*Barrantes and Madsen*, 2000]. However, the effect of bedform orientation and lengthscales in the surfzone with combined wave–current flows is not understood. Thus, as in *Garcez-Faria et al.* [1998], the relationship between bedform height and c_d is investigated, and the effects of bedform lengthscales and orientation while potentially significant are not considered.

Drag Coefficient Estimates

Drag coefficient estimates are based on a 1-D alongshore momentum balance between wind and wave forcing, bottom stress, and lateral mixing given by

$$\tau_y^{\text{wind}} - \frac{dS_{xy}}{dx} = \rho c_d \langle |\vec{u}|v \rangle + \frac{dM_{xy}}{dx}, \quad (5)$$

where τ_y^{wind} is the alongshore (y) wind stress. Cross-shore (x) derivatives of S_{xy} and M_{xy} , components of the radiation and depth-integrated lateral Reynolds stresses [e.g., *Svendsen and Putrevu, 1994*], respectively, are difficult to estimate with observations. However, the observations can be used to estimate cross-shore integrals of terms in (5), from which spatially-averaged surfzone and seaward of the surfzone c_d can be calculated.

The c_d within and seaward of the surfzone are calculated by integrating (5) over the entire 750-m long current meter transect from approximately the shoreline ($x = 0$) to 8-m water depth ($x = x_{8m}$) [*Feddersen et al., 1998*]. The cross-shore integration is separated into two components, one spanning the surfzone and one seaward of the surfzone. In 8-m water depth, usually well seaward of the surfzone, pressure array data and linear theory are used to estimate S_{xy} , and the Reynolds stress M_{xy} is assumed negligible. At $x = 0$, the location of the most shoreward instrument, S_{xy} and M_{xy} are set equal to zero. Swash processes onshore of the most shoreward current meter are thus assumed to contribute negligibly to the cross-shore integrated, alongshore momentum balance. This assumption is consistent with standard models for radiation (based on depth-limited wave breaking) and Reynolds stresses, and is supported by the closure of an integrated alongshore momentum balance that neglects the swash region [*Feddersen et al., 1998*]. Although c_d may vary continuously in the cross-shore,

c_d is assumed spatially constant within each the surfzone and seaward of the surfzone regions, and c_d is passed through the integrals. With a spatially constant wind stress, the cross-shore integral of (5) becomes,

$$\tau_y^{\text{wind}} \cdot x_{8m} - S_{xy}|_{x_{8m}} = \rho c_{d1} \int_0^{x_b} \langle |\vec{u}|v \rangle dx + \rho c_{d2} \int_{x_b}^{x_{8m}} \langle |\vec{u}|v \rangle dx, \quad (6)$$

where x_b is the location of the breakpoint. The unknown drag coefficients within and seaward of the surfzone are represented by c_{d1} and c_{d2} , respectively. Observed 2-Hz velocity time series are used to estimate $\langle |\vec{u}|v \rangle$ at each current meter. Hourly estimates of the total forcing, and surfzone and seaward integrated $\langle |\vec{u}|v \rangle$ are linearly regressed to calculate 48-hr values of best-fit c_d within and seaward of the surfzone (see *Feddersen et al.* [1998] for details).

The selected 48-hr time interval is a compromise between long time intervals needed for statistical stability of the c_d estimates, and short-time intervals that better resolve temporal variability of k_{rms} , c_d , and the cross-shore extent of the surfzone. The results were similar using 24- and 48-hr averaging intervals. Successive hourly estimates of integrated $\langle |\vec{u}|v \rangle$ (and of the total forcing) are not independent [*Feddersen et al.*, 1998], and thus the effective degrees of freedom and confidence limits for each 48-hr c_d estimate cannot be determined. To eliminate inaccurate estimates, 48-hr c_d values were rejected if the regression had poor skill (defined as skill < 0.4) or if c_d was negative.

3. Relationship Between the Drag Coefficient, Roughness, and Wave

Breaking

Table 1.

Estimates of c_d , k_{rms} , and k_{rms}/h are consistently larger in the surfzone than seaward of the surfzone (compare circles with crosses in Figure 4). The average surfzone c_d is significantly ($> 99\%$ confidence) larger than the average c_d seaward of the surfzone, consistent with c_d estimated using a single regression for the entire 2-month period (dashed lines in Figure 4), but roughly a factor of two less than the equivalent c_d derived from friction factors cited by *Nielsen et al.* [2001].

A relationship between k_{rms} and c_d (Figure 4a) and k_{rms}/h and c_d (Figure 4b) is apparent when the regions within and seaward of the surfzone are considered together. However, this is misleading because considering both regions together does not control for other factors that could effect c_d such as breaking-wave generated turbulence.

Figure 4.

To isolate the effect of enhanced turbulence due to bottom roughness from turbulence due to breaking waves, the relationship between roughness quantities and c_d is examined separately within and seaward of the surfzone. Within the surfzone, no relationship is observed between k_{rms} and c_d (circles in Figure 4a), nor between k_{rms}/h and c_d (circles in Figure 4b). The correlations (Table 1) are not significant at the 90% confidence level. The lack of a detectable c_d dependence on spatially averaged k_{rms} or k_{rms}/h suggests that roughness quantities are not the critical factor determining the surfzone c_d .

Seaward of the surfzone the correlation between k_{rms} and c_d ($r = 0.33$, Table 1, crosses in Figure 4a) is increased relative to the correlation within the surfzone, but is not significant

at the 90% level, suggesting that k_{rms} alone is not responsible for the c_d variation seaward of the surfzone. However, the correlation ($r = 0.47$, Table 1) between seaward of the surfzone k_{rms}/h and c_d is significant at the 90% level (crosses in Figure 4b). This is consistent with the hypothesis that c_d seaward of the surfzone depends on the depth-normalized apparent roughness k_a/h , because k_a is a function of the physical roughness [Grant and Madsen, 1979].

4. Discussion

The consistently elevated surfzone c_d over a broad range of roughness (Figure 4) implies that other surfzone processes, such as wave breaking, are important to c_d . However, this conclusion is tentative due to limitations of the data and analysis methods. These limitations include the inability to estimate bed roughness more frequently than every 24 hours because bedforms migrate slowly past the altimeter (Figure 2). Using 24-hr averaged roughness quantities and breakpoint locations can degrade roughness estimates within and seaward of the surfzone by including observations from locations sometimes outside each region when there is a rapid change in surfzone width. Also, the instantaneous bed roughness is spatially patchy [Gallagher *et al.*, 2002], which is obscured with a 24-hr averaged k_{rms} . The potential effect of variable bedform lengths and orientations [Barrantes and Madsen, 2000] were not taken into account. In addition, the estimated correlation between c_d and roughness will be reduced below the true correlation if c_d and roughness vary over the 48-hr averaging time necessary to obtain statistical stability.

The result that c_d does not depend on roughness in the surfzone differs from the (log profile based) result of Garcez-Faria *et al.* [1998]. A requirement of log-profile models (3)

is that the bottom boundary layer is a constant stress layer where shear production balances turbulent dissipation ϵ , yielding a dissipation scaling

$$\epsilon = \frac{\overline{v_*^3}}{\kappa z} \quad (7)$$

where ϵ decreases with height z above the bed. This dissipation scaling (7) is consistent with measurements (for example) on the Northern California continental shelf [Grant *et al.*, 1984] and the Hudson River Estuary [Trowbridge *et al.*, 1999]

In the shallow water of the surfzone, breaking-wave generated turbulence can penetrate the entire water column. For example, laboratory observations show increased turbulence associated with wave breaking within 0.3 cm of the bed [Cox and Kobayashi, 2000]. Surfzone dissipation observed in the field [George *et al.*, 1994] is 10^2 to 10^3 times larger than the near-bottom dissipation observed in a tidal estuary [Trowbridge *et al.*, 1999], and does not decay as z^{-1} (7), but increases with height above the bed. Laboratory measurements of surfzone turbulent kinetic energy q show a maximum at mid-water column [Ting and Kirby, 1994]. If $\epsilon \sim q^{3/2}$, as commonly is assumed in the surfzone [e.g., Svendsen, 1987], the laboratory surfzone ϵ also increases with height above the bed.

These (and other) laboratory and natural surfzone observations suggest that the dissipation scaling (7) likely is not applicable in the surfzone. Thus, mean bottom stress (and therefore c_d) inferred by fitting mean currents to a log profile may be incorrect. Similarly, the concept of an apparent roughness k_a [e.g., Grant and Madsen, 1979] also is not applicable to the surfzone, and the relationship between k_a and c_d therefore is not investigated.

5. Conclusions

Observations along a cross-shore transect of current meters and altimeters extending 750 m from the shoreline to 8-m water depth show that the drag coefficient c_d and bottom roughness k_{rms} are larger inside the surfzone than outside the surfzone. No dependence of c_d on k_{rms} or k_{rms}/h is found within the surfzone, nor between c_d and k_{rms} seaward of the surfzone. There is a weak relationship between c_d and k_{rms}/h seaward of the surfzone, consistent with the hypothesis that k_{rms}/h influences c_d when waves are not breaking. Although the data and methods have limitations, the lack of an observed relationship between c_d and roughness, together with the existing evidence of increased surfzone turbulence dissipation associated with breaking waves, suggest that breaking-wave generated turbulence leads to increased surfzone c_d .

Acknowledgments. The instrument array was deployed and maintained by staff from the Center for Coastal Studies. Tom Herbers and Britt Raubenheimer helped collect and process the data. Excellent logistical support and the 8-m depth pressure sensor array data were provided by the U.S. Army Corps of Engineers Field Research Facility. Steve Lentz provided the wind stress data. We have benefited from discussions with John Trowbridge, Tony Bowen, Rob Holman, and an anonymous reviewer. This research was funded by the Office of Naval Research, the National Science Foundation, the National Ocean Partnership Program, and the Army Research Office. Woods Hole Oceanographic Institution contribution 10286.

References

- Barrantes, A. I., and O. S. Madsen, Near-bottom flow and flow resistance for currents obliquely incident to two-dimensional roughness elements, *J. Geophys. Res.*, *105*, 26,253–26,264, 2000.
- Church, J. C., and E. B. Thornton, Effects of breaking wave induced turbulence within a longshore current model, *Coastal Eng.*, *20*, 1–28, 1993.
- Cox, D. T., and N. Kobayashi, Identification of intense, intermittent coherent motions under shoaling and breaking waves, *J. Geophys. Res.*, *105*, 14,223–14,236, 2000.
- Feddersen, F., R. T. Guza, S. Elgar, and T. H. C. Herbers, Alongshore momentum balances in the nearshore, *J. Geophys. Res.*, *103*, 15,667–15,676, 1998.
- Feddersen, F., R. T. Guza, S. Elgar, and T. H. C. Herbers, Velocity moments in alongshore bottom stress parameterizations, *J. Geophys. Res.*, *105*, 8673–8686, 2000.
- Fredsoe J., and R. Deigaard, *Mechanics of Coastal Sediment Transport*, World Sci., River Edge, N. J., 1992.
- Gallagher, E. L., W. Boyd, S. Elgar, R. T. Guza, and B. Woodward, Performance of a sonar altimeter in the nearshore, *Mar. Geol.*, *133*, 241–248, 1996.
- Gallagher, E. L., S. Elgar, and R. T. Guza, Observations of sand bar evolution on a natural beach, *J. Geophys. Res.*, *103*, 3203–3215, 1998a.
- Gallagher, E. L., S. Elgar, and E. B. Thornton, Megaripple migration in a natural surf zone, *Nature*, *394*, 165–168, 1998b.
- Gallagher, E. L., E. B. Thornton, T. P. Stanton, Sand bed roughness in the nearshore, *J. Geophys. Res.*, in press, 2002.

- Garcez-Faria, A. F., E. B. Thornton, T. P. Stanton, C. M. Soares, and T. C. Lippmann, Vertical profiles of longshore currents and related bed shear stress and bottom roughness, *J. Geophys. Res.*, *103*, 3217–3232, 1998.
- George, R., R. E. Flick, and R. T. Guza, Observations of turbulence in the surf zone, *J. Geophys. Res.*, *99*, 801–810, 1994.
- Grant, W. D., and O. S. Madsen, Combined wave and current interaction with a rough bottom, *J. Geophys. Res.*, *84*, 1797–1808, 1979.
- Grant, W. D., A. J. Williams, and S. M. Glenn, Bottom stress estimates and their prediction on the Northern California continental shelf during CODE-1: The importance of wave current turbulence, *J. Phys. Oceanogr.*, *14*, 506–527, 1984.
- Longuet-Higgins, M. S., Longshore currents generated by obliquely incident sea waves 1, *J. Geophys. Res.*, *75*, 6790–6801, 1970.
- Nielsen, P., R. W. Brander, and M. G. Hughes, Rip currents: Observations of hydraulic gradients, friction factors, and wave pump efficiency, *Proc. Coastal Dynamics '01*, Lund, Sweden, p. 489, 2001.
- Özkan-Haller, H. T., and J. T. Kirby, Nonlinear evolution of shear instabilities of the longshore current: A comparison of observations and computations, *J. Geophys. Res.*, *104*, 25,953–25,984, 1999.
- Svendsen, I. A., Analysis of surf zone turbulence, *J. Geophys. Res.*, *92*, 5115–5124, 1987.
- Svendsen, I. A., and U. Putrevu, Nearshore mixing and dispersion, *Proc. Royal Soc. Lond. A*, *445*, 561–576, 1994.
- Ting, F. C. K., and J. T. Kirby, Observations of undertow and turbulence in a laboratory surfzone, *Coastal Eng.*, *24*, 51–80, 1994.

Thornton, E. B., J. L. Swayne, and J. R. Dingler, Small-scale morphology across the surf zone, *Mar. Geol.*, 145, 173–196, 1998.

Trowbridge, J. H., W. R. Geyer, M. M. Bowen, and A. J. Williams, Near-bottom turbulence measurements in a partially mixed estuary: Turbulent energy balance, velocity structure, and along-channel momentum balance, *J. Phys. Oceanogr.*, 29, 3056–3072, 1999.

Van Rijn, L. C., *Principles of Sediment Transport in Rivers, Estuaries, and Coastal Seas*, Aqua Publications, Netherlands, 1993.

F. Feddersen and S. Elgar, Woods Hole Oceanographic Institution, AOPE MS#12, Woods Hole, MA, 02543. (e-mail: falk@whoi.edu; elgar@whoi.edu)

R. T. Guza, Center for Coastal Studies Scripps Institution of Oceanography, University of California, La Jolla, CA 92093-0209. (e-mail: rguza@ucsd.edu)

E. L. Gallagher, Dept. of Oceanography, Naval Postgraduate School, Monterey, CA 93943-5122 (e-mail: egallagh@oc.nps.navy.mil)

Received _____

March 17, 2003

This manuscript was prepared with AGU's \LaTeX macros v5, with the extension package 'AGU++' by P. W. Daly, version 1.6b from 1999/08/19.

Figure Captions

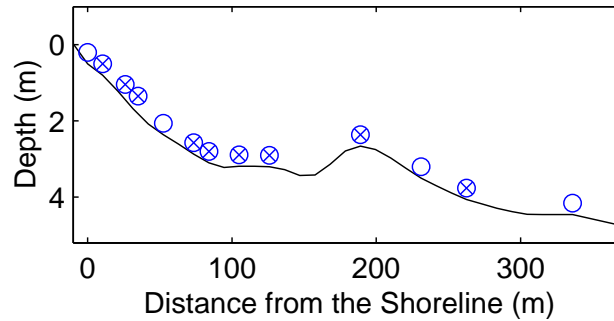


Figure 1. Depth versus distance from the shoreline (solid curve) on August 25, 1994, and locations of current meters (circles) and altimeters (crosses). An additional current meter and the pressure sensor array were located 750 m from the shoreline in approximately 8-m water depth.

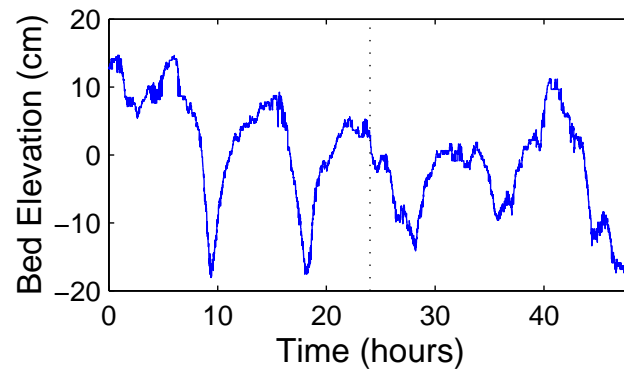


Figure 2. Demeaned 32-s bed elevation versus time for a 48-hr period. The k_{rms} is 6.9 and 4.5 cm for the first and second 24-hr periods, respectively.

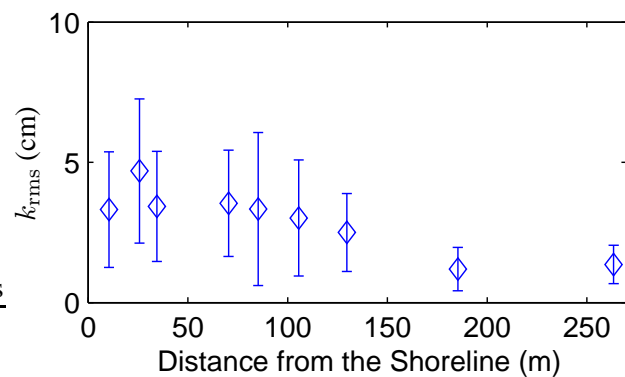


Figure 3. Mean (diamonds) and standard deviation (vertical bars) of k_{rms} versus distance from the shoreline. There are between 53 and 58 24-hr observations at each location. The mean for all 511 24-hr observations is 2.9 cm, the standard deviation is 2.2 cm, and the largest observed k_{rms} is 10.7 cm.

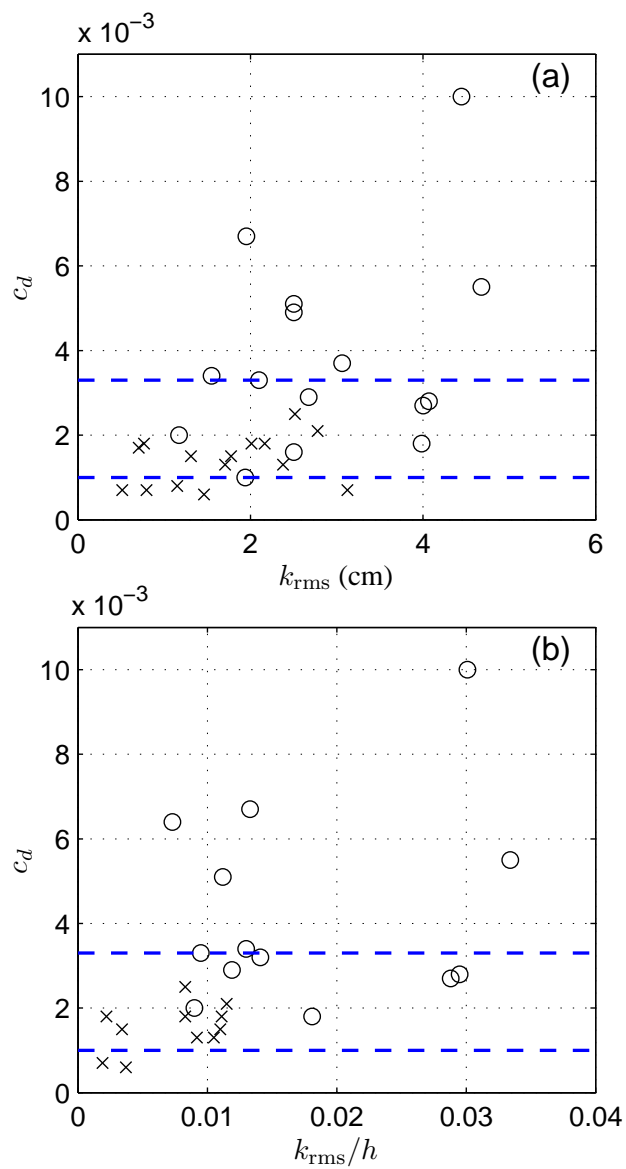


Figure 4. (a) c_d versus k_{rms} and (b) c_d versus k_{rms}/h for the surfzone (circles) and seaward of the surfzone (crosses). The upper and lower dashed lines in each panel are the surfzone and seaward of the surfzone two-month best-fit c_d , respectively [Fedderson *et al.*, 1998]. Statistics are presented in Table 1.

Tables

Table 1. Correlation r between drag coefficient c_d and both bottom roughness k_{rms} and normalized bottom roughness k_{rms}/h . The number of data points in each correlation is N .

	Seaward of the			
	Surfzone		Surfzone	
	N	r	N	r
k_{rms}	17	0.27	15	0.33
k_{rms}/h	13	0.23	11	0.47 [†]

[†]Correlation significant ($\neq 0$) with 90% confidence